



# Xuanbai Chengqi Decoction Ameliorates Pulmonary Inflammation via Reshaping Gut Microbiota and Rectifying Th17/Treg Imbalance in a Murine Model of Chronic Obstructive Pulmonary Disease

Yongan Wang <sup>1,\*</sup>


Na Li <sup>1,\*</sup>


Qiuyi Li <sup>1</sup>

Zirui Liu <sup>1</sup>

Yalan Li <sup>1</sup>

Jingwei Kong <sup>1</sup>

Ruijuan Dong <sup>2</sup>

Dongyu Ge <sup>2</sup>

Jie Li <sup>3</sup>

Guiying Peng <sup>1</sup>

<sup>1</sup>Department of Immunology and Microbiology, School of Life Sciences, Beijing University of Chinese Medicine, Beijing, People's Republic of China;

<sup>2</sup>Experimental Teaching Center, School of Traditional Chinese Medicine, Beijing University of Chinese Medicine, Beijing, People's Republic of China; <sup>3</sup>Department of Respiratory Medicine, Dongzhimen Hospital, Beijing University of Chinese Medicine, Beijing, People's Republic of China

\*These authors contributed equally to this work

**Purpose:** Chronic obstructive pulmonary disease (COPD), a prevalent obstructive airway disease, has become the third most common cause of death globally. Xuanbai Chengqi decoction (XBCQ) is a traditional Chinese medicine prescription for the acute exacerbation of COPD. Here, we aimed to reveal the therapeutic effects of XBCQ administration and its molecular mechanisms mediated by Th17/Treg balance and gut microbiota.

**Methods:** We determined the counts of Th17 and Treg cells in the serum of 15 COPD and 10 healthy subjects. Then, cigarette smoke extract-induced COPD mice were gavaged with low, middle, and high doses of XBCQ, respectively. Weight loss, pulmonary function and inflammation, Th17/Treg ratio, and gut microbiota were measured to evaluate the efficacy of XBCQ on COPD.

**Results:** COPD patients had a higher Th17/Treg ratio in the serum than healthy controls, which was consistent with the results in the lung and colon of COPD mice. The middle dose of XBCQ (M-XBCQ) significantly decreased the weight loss and improved the pulmonary function (FEV<sub>0.2</sub>/FVC) in COPD mice. Moreover, M-XBCQ alleviated lung inflammation by rectifying the Th17/Treg imbalance, reducing the expressions of TNF- $\alpha$ , IL-1 $\beta$ , and MMP-9, and suppressing inflammatory cells infiltration. Meanwhile, M-XBCQ greatly improved the microbial homeostasis in COPD mice by accumulating probiotic *Gordonibacter* and *Akkermansia* but inhibiting the growth of pathogenic *Streptococcus*, which showed significant correlations with pulmonary injury.

**Conclusion:** Oral M-XBCQ could alleviate COPD exacerbations by reshaping the gut microbiota and improving the Th17/Treg balance, which aids in elucidating the mechanism through which XBCQ as a therapy for COPD.

**Keywords:** XBCQ, COPD, intestinal microbiota, Th17/Treg, pulmonary inflammation

## Introduction

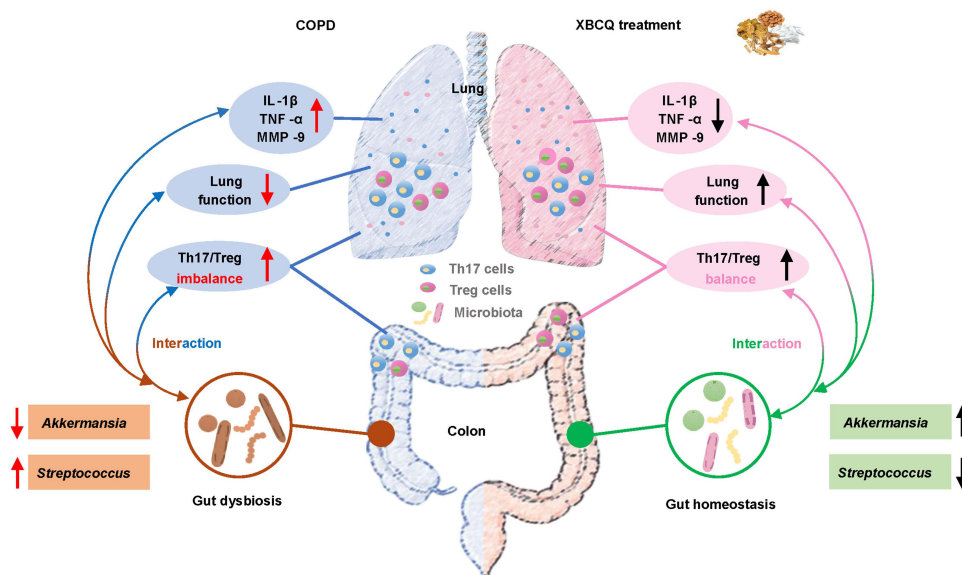
COPD is an obstructive airway disease clinically characterized by emphysema and/or persistent bronchitis, leading to non-reversible airway obstruction, pulmonary inflammation, and lung injury. COPD has become the third most common cause of death globally, and its main risk factors can be attributed to cigarette smoking and air pollution.<sup>1,2</sup> At present, long-acting bronchodilators primarily including long-acting

Correspondence: Guiying Peng; Jie Li  
Email penggy@bucm.edu.cn;  
lijie2007@126.com

Received: 1 September 2021  
Accepted: 22 November 2021  
Published: 7 December 2021



## Graphical Abstract



$\beta$ 2-agonists muscarinic antagonists, usually in combination with glucocorticoids, have been widely employed in the treatment of COPD.<sup>3</sup> However, these therapies are limited in targeting the underlying disease process, reducing disease mortality, or reversing tissue damage, followed by unacceptable side effects.<sup>4</sup> Further studies are needed to figure out the mechanism of pulmonary inflammation and lung injury in association with COPD and to develop new safe and efficient anti-inflammatory drugs.

Increasing evidence indicates that the Th17 and Treg balance plays vital roles in regulating the pathogenesis of COPD.<sup>5</sup> Th17 cells are a subset of pro-inflammatory T helper cells responsible for producing IL-17A and IL-17F, which are closely linked to neutrophilic inflammation.<sup>6</sup> However, Treg cells are a unique subset of regulatory T cells, defined as CD4<sup>+</sup>CD25<sup>+</sup>Foxp3<sup>+</sup> T cells, which maintain immune homeostasis by secreting IL-10 and TGF- $\beta$ .<sup>7</sup> A previous study has proved that compared to control subjects, Th17-related cytokines are prominently increased in the bronchial mucosa of stable COPD patients.<sup>8</sup> Meanwhile, these cytokines can induce epithelial cells to produce antimicrobial peptides, chemokines, and granulocyte growth factors such as G-CSF and GM-CSF, thereby promoting the accumulation of neutrophils.<sup>9</sup> Cigarette smokers with COPD exhibited fewer Treg cells, lower mRNA levels for Foxp3, and less

IL-10 secretion in the whole lung than controls.<sup>10</sup> At the same time, the density of Treg cells in COPD patients fluctuated in bronchoalveolar lavage or lung tissue.<sup>11</sup> Moreover, Cervilha et al demonstrated the critical role of Th17/Treg imbalance worsening the pulmonary inflammation using a cigarette smoke extract (CSE)-challenged COPD mice model.<sup>12</sup>

The gastrointestinal tract (GIT) harbors a complex and diverse microbial community that is paramount for sustaining the ecological equilibrium with the host immune system.<sup>13,14</sup> In the meantime, the dysbiosis of the gut microbiome is believed to be closely connected with a higher risk of diseases and infections.<sup>15</sup> Different bacterial species can induce distinct immune cell populations with pro- or anti-inflammatory effects, in which case a normal gut ecosystem contributes more to protecting against the susceptibility to inflammatory infections and diseases.<sup>16</sup> In recent years, many studies have revealed that lung microbiome imbalance is another contributing factor to the progression of COPD.<sup>17,18</sup> Along with the intimate relationship between GIT and the respiratory tract, the “gut-lung axis” might be very important for COPD pathogenesis.<sup>19</sup> A novel study indicated that the gut microbiome and metabolome of COPD patients are significantly distinguished from those of healthy subjects.<sup>4</sup> Similar observations have also been replicated in cigarette

smoking-based murine models with COPD, again confirming the potential role of the gut microbiome in exacerbating lung inflammation.<sup>20,21</sup> Therefore, the gut microbiota intervention would be a potential therapeutic approach for the prevention and treatment of COPD. Besides, accumulating evidence has shown that the mucosal microbiota could regulate the Treg/Th17 balance by secreting functional metabolites such as short-chain fatty acids, thus governing immune homeostasis.<sup>22,23</sup> In this case, we hypothesized that this interaction between resident microbiota and Th17/Treg balance might be further involved in regulating the occurrence and exacerbation of COPD.

Xuanbai Chengqi decoction (XBCQ) is a representative Chinese medicine prescription in Systematized Identification of Warm Diseases written by Wu Jutong in the Qing dynasty. XBCQ has been widely used to treat a variety of common respiratory diseases in China, such as lung injury, lung fibrosis, and COPD.<sup>24–27</sup> XBCQ can serve as an effective remedy for resolving phlegm, expelling heat by purgation, as well as alleviating cough, wheezing, and chest congestion, with little adverse reactions,<sup>25,28</sup> which is therefore generally prescribed for COPD. As well, a clinical study found that the XBCQ medication could produce a significant improvement in the oxidant/antioxidant imbalance, damaged lung function, and excessive inflammatory responses of COPD patients.<sup>25</sup> This traditional remedy consists of four constituents, namely, rhubarb, gypsum, apricot seed, and trichosanthes rind.<sup>25</sup> In addition, amygdalin from apricot seed has inhibitory activity during the epithelial-mesenchymal transitions process in COPD mice.<sup>29</sup> However, the underlying molecular mechanism by which XBCQ ameliorates pulmonary inflammation remains poorly understood.

In the present study, we for the first time compared the difference in the Th17/Treg balance between clinical subjects with or without COPD. Then, we explored the efficacy of XBCQ on pulmonary inflammation and lung injury using an experimental murine model of COPD. The mechanisms by which XBCQ improved the deterioration of COPD mediated by Th17/Treg balance and gut microbiota were also disclosed. Cigarettes are considered as one of the most prevalent risk factors for clinical COPD,<sup>30,31</sup> which are therefore the most commonly used harmful gas to mimic COPD. Extensive investigations have applied the exposure of cigarette smoke (CS) combined with LPS to generate a COPD murine model.<sup>32–34</sup> This kind of COPD model can effectively reproduce the

airway phenotype of clinical patients with COPD and induce a significant rise in the secretion of pro-inflammatory cytokines, such as TNF- $\alpha$  and IL-1 $\beta$ .<sup>33</sup> Besides, compared with the simple CS-induced COPD models, the combination of CS and LPS can obtain more similar pathological features to human COPD and also exhibit a shorter modeling time. Therefore, based on these previous studies, our study finally selected and established the COPD model by the nasal inhalation with CSE combined with LPS. The findings of this study will facilitate the exploration of new therapeutic biomarkers and adjuvant medication for patients with COPD.

## Materials and Methods

### Human Participants and Specimen Collection

A total of 15 COPD patients and 10 healthy subjects were recruited from Dongzhimen Hospital, Beijing University of Chinese Medicine (Beijing, China). Inclusion criteria for COPD participants: (1) Meet the diagnostic criteria of the guidelines from the Global Initiative for Chronic Obstructive Lung Disease (GOLD 2020); (2) FEV1/FVC < 70% after inhaling bronchodilators, except for other pulmonary diseases; (3) Aged 18 to 75 years old, but the gender was not limited; (4) Signed informed consent was provided. Inclusion criteria for healthy subjects: (1) Healthy body without chronic wasting diseases; (2) Without chronic respiratory diseases; (3) Aged 18 to 75 years old, but the gender was not limited; (4) Signed informed consent was provided. Besides, we excluded participants who had received antibiotic or prednisone treatments during the last two months or had a prior history of gastrointestinal disease. Serum samples from all participants were collected and stored at  $-80^{\circ}\text{C}$  until measurement. This study was performed according to the principles of the Declaration of Helsinki and was approved by local human research ethics committees. All subjects were provided written informed consent, and all protocols were approved by the Ethics Committee of Dongzhimen Hospital Affiliated with Beijing University of Chinese Medicine (reference 2020DZMEC-093-02).

### Preparation of XBCQ and CSE

The constitution of XBCQ is shown in Table 1. Four herbs were purchased from Beijing Tong-Ren-Tang (Beijing, China). All herbs were boiled twice, 10 min with high heat and then 20 min with gentle heat after soaking for 30

**Table 1** Components of XBCQ Prescription

Component of XBCQ	Chinese Name	Origin	Amount (g)
<i>Rheum officinale</i> Baill	Sheng Da Huang	Dried roots and rhizomes	9
<i>Gypsum Fibrosum</i>	Sheng Shi Gao	Mineral gypsum	15
<i>Prunus armeniaca</i> L.	Ku Xing Ren	Dried mature seed	6
<i>Trichosanthes kirilowii</i> Maxim	Gua Lou Pi	Dried ripe peel	4.5
Total			34.5

min. The decoction was filtered with two-layer gauze to remove residue and then heated to a concentration of 1.15 g/mL.<sup>26</sup> The decoction was aliquoted and stored at  $-80^{\circ}\text{C}$ . The commercial non-filtered cigarettes were purchased from Zhongnanhai from the Beijing cigarette factory (Beijing, China). Each cigarette contained 10 mg of tar, 0.9 mg of nicotine, and 10 mg of CO. CSE was prepared according to Su et al.<sup>35</sup> Briefly, the mainstream smoke from 3 cigarettes was drawn by a vacuum pump using 30 mL of pre-warmed PBS. The pH of the solution was adjusted to 7.2–7.4 and then filtered with a 70  $\mu\text{m}$  sterile cell strainer after the smoke was sufficiently dissolved. All CSE was aliquoted and stored at  $-80^{\circ}\text{C}$ .

## HPLC Analysis of XBCQ

We first performed the initial batch-to-batch consistency studies using high-performance liquid chromatography (HPLC) to characterize the main components in the XBCQ decoction. In brief, the XBCQ decoction was lyophilized to powder and then dissolved in the methanol. After filtration (0.22  $\mu\text{m}$ ), the samples were injected into the HPLC system and then separated on the chromatographic column C18 (A6000100R046, Agilent, U.S.A). The following conditions were used for HPLC: flow phase: A: acetonitrile, B: 0.1% phosphoric acid water, 0–20 min, A: 4%–7%; 20–25 min, A: 7%–9%; 25–45 min, A: 9%–11%; 45–55 min, A: 11%–14%; 55–80 min, A: 14%–18%; 80–120 min, A: 18%–52%; 120–130 min, A: 52%–70%; 130–135 min, A: 70%; 135–140 min, A: 70%–75%; detection wavelength: 0–40 min, 215 nm; 40–80 min, 25 nm; 80–110 min, 320 nm; 110–140 min, 254 nm.

## Experimental Mouse Model of COPD and Drug Administration

To reveal the mechanisms of XBCQ ameliorating COPD, we constructed a mouse model with COPD by the intranasal administration with CSE and LPS according to Amano et al with slight modifications.<sup>36</sup> A total of 48 female C57BL/6

mice at 6–8 weeks of age were purchased from Beijing Vital River Laboratory Animal Technology Company (Beijing, China). All mice had free access to pathogen-free food and water on a 12 hr light-dark cycle (25  $^{\circ}\text{C}$ ). All animal experiments were performed in the Animal Management Centre of Beijing University of Chinese Medicine with qualification certificate SYXK (Beijing) 2020–0033. All animal studies were approved by the Animal Ethics Committee of Beijing University of Chinese Medicine (BUCM-4-2018062901-2062) and performed according to the guidelines of the Beijing University of Chinese Medicine Animal Care and Use Committee.

After one-week adaptation feeding, mice were randomly divided into six groups ( $n = 4\text{--}8$  mice/group): Negative control group, COPD group, COPD with low, middle, and high doses of XBCQ groups (L-XBCQ, M-XBCQ, and H-XBCQ), and positive control group with dexamethasone (DEX). Except for the negative control group, experimental COPD was induced in all the other treatments. In brief, on 0–4 and 7–11 days at the beginning of this trial, mice were intranasally administered with CSE (25  $\mu\text{L}/\text{mouse}$ ) and LPS (25  $\mu\text{L}/\text{mouse}$ , Sigma-Aldrich Co.Ltd) after isoflurane inhalation. On days 14–18 mice were given only CSE. Mice in the control group were administered with sterile PBS.

On days 21 to 27, four treatments with COPD were intragastrically gavaged by low (0.35 g/mL), middle (0.7 g/mL), and high (1.4 g/mL) doses of XBCQ, as well as DEX (2 mg/kg, Shanghai Yuanye Bio-Technology Co., Ltd) once a day (200  $\mu\text{L}/\text{mouse}$ ), respectively. The middle dose of XBCQ was determined by calculating the clinical equivalent dose using a conversion coefficient from human to mouse based on body surface area, as instructed by multiple previous studies.<sup>37,38</sup> The low- and high-dose of XBCQ were 1/2 or 2 times of the medium concentration, respectively. The detailed calculation formula based on the standard body weight of adults and mice is as follows:

“Clinical equivalent dose of one mouse (M-XBCQ, g/mL)



= (clinical dose × conversion coefficient × body weight of mice)/gavage volume

= (34.5 g/60 kg × 12.3×0.02 kg)/0.2 mL = 0.7 g/mL.”

Mice in another two groups were administered with sterile PBS. All the mice were euthanized at 28 days by intraperitoneal injection with 100 mg/kg sodium pentobarbital, and colonic digesta and lung tissues were collected for further analysis. The timeline of this test is shown in Figure 1.

## Assessment of Pulmonary Function

We next measured the pulmonary function of CSE and LPS-treated mice to determine the occurrence of airway inflammation. The AniRes 2005 lung system (Bestlab, AniRes 2005, version 2.0, China) was used to detect pulmonary function before the execution with all operations performed according to the manufacturer’s instructions. Mice were anesthetized by pentobarbital sodium and connected to a computer-controlled animal ventilator through a tracheal cannula. The respiratory rate and the time ratio of expiration/inspiration were preset at 95/min and 1.5:1, respectively. Data were recorded, and the FEV<sub>0.2</sub>/FVC ratio used as the criterion for determining the lung function<sup>33</sup> was analyzed by the software provided by the AniRes 2005 lung system.

## Pulmonary Histopathological Examination

Lung tissues were washed in phosphate buffer and fixed in 4% formaldehyde at room temperature, dehydrated in the graded concentration of ethanol, and then embedded in paraffin. Tissue sections of 4 μm thickness were stained with hematoxylin and eosin (H&E) for the histopathological examination. Digital images of pulmonary morphology at 200× magnification were obtained using a light microscope.

## Immunohistochemistry Analysis of Lung Tissues

Immunohistochemistry (IHC) was used to detect the expression of matrix metalloproteinases-9 (MMP-9) which is critical to the process of lung inflammation. Following deparaffinization and rehydration, lung sections were incubated with 0.01 M citrate buffer for 15 min in 95 °C water and rinsed with PBS three times for 5 min. Tissue sections were incubated with primary antibody incubation anti-mouse MMP-9 antibody (BioLegend, Inc., U.S.A) overnight at 4 °C and then rinsed 5 min three times with PBS. The next day, Horseradish Peroxidase-labeled secondary antibody (Zsbio Commerce Store, China) was incubated with sections for 20 min at 37 °C and rinsed with PBS for 5 min three times. Ten visual fields at 200× magnification were randomly selected for each sample, and their integral optical density (IOD) was measured using Image-Pro software.

## RNA Isolation, cDNA Synthesis, and Real-Time Quantitative PCR

Total RNA from lung tissues was extracted using Trizol reagent (Sigma-Aldrich, Germany). RNA was quantified by a Nanodrop ND-1000 Spectrophotometer (Thermo Fisher Scientific, U.S.A) and then reverse transcribed into cDNA using QuantiNova Reverse Transcription Kit (Qiagen Ltd., Germany). RT-qPCR was performed in a QuantStudio6 Flex system (Life Technologies, U.S.A) with miScript SYBR Green PCR Kit (Qiagen Ltd., Germany). The mRNA expressions of targeted genes were normalized using a housekeeping control (GAPDH) and calculated by the  $2^{-\Delta\Delta Ct}$  method. Specific primers used in this study were as follows: 5’-

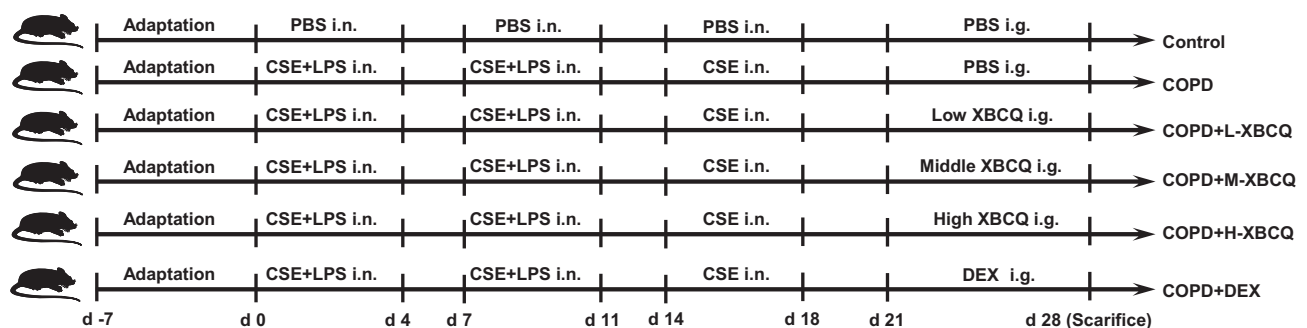


**Figure 1** The timeline of the animal test.

**Abbreviations:** COPD, chronic obstructive pulmonary disease; CSE, cigarette smoke extract; L-XBCQ, the low dose of XBCQ; M-XBCQ, the middle dose of XBCQ; H-XBCQ, the high dose of XBCQ; DEX, dexamethasone.

CTTCTCATTCTGCTTGTGGC-3'/5'-CCACTTGGTGGT TTGTGAGTG-3' for TNF- $\alpha$ ; 5'-CAGCAACAGCAAGG CGAAAA-3'/5'-CGCTTCTGAGGCTGGATTC-3' for IFN- $\gamma$ ; 5'-AATGCCACCTTTTGACAGTGATG-3'/5'-CCTGC CTGAAGCTCTTGTTG-3' for IL-1 $\beta$ .

## Isolation of Human Peripheral Blood Mononuclear Cells (PBMCs) and Lymphocytes from Lung and Colonic Tissues

Venous blood was collected from all participants. PBMCs were isolated from the whole blood using Human PBMC Separation Medium (TBD Science, China), centrifuged (Eppendorf, Germany) following the manufacturer's instruction (TBD Science, China), and resuspended in PBS with 0.5% BSA.

For the isolation of lymphocytes from the lung and colon, the single-cell suspension was obtained according to a previous study.<sup>39</sup> Fresh lung tissues were minced and incubated with 1 mg/mL collagenase IV (Worthington, USA) and 50  $\mu$ g/mL DNase I (Roche, Switzerland) in RPMI-1640 media (Biological Industries, Israel) before being mashed through 70  $\mu$ m cell strainers. After removing adherent fat tissue and Peyer's patches, the colon was washed twice with 20 mL HBSS medium containing 5 mM EDTA and 1 mM DTT to remove epithelial cells. Next, 2 mg/mL collagenase type III (Worthington, USA) and 50  $\mu$ g/mL DNase I (Roche, Switzerland) in RPMI-1640 media were used to digest colon tissues. The digested tissues were filtered through 70  $\mu$ m cell strainers to obtain cell suspension and enriched with a 40% Percoll gradient after red blood cells were lysed. PBMCs and single-cell suspensions from all tissues were used for subsequent flow cytometry staining.

## Flow Cytometry Analysis for Th17 and Treg Cells

Isolated human PBMCs suspension was separated into two parts to be stained. All staining of molecules with fluorescently labeled antibodies was performed in the dark. All antibodies were purchased from Biolegend Ltd., U. S. A. For the Treg staining, cells were stained with APC anti-human CD3, FITC-conjugated anti-human CD4, AF700 anti-human CD8, and BV421 anti-human Foxp3 for 30 min in 4 °C, followed by using Invitrogen Fixation/Permeabilization Concentrate (eBioscience, U.S.A) to fix and permeabilize cells. Then, cells were stained with PE

anti-human CD25. For the Th17 staining, cells were treated with Cell Stimulation Cocktail for 6 h at 37 °C before being stained with APC anti-human CD3, FITC-conjugated anti-human CD4, AF700 anti-human CD8 for 30 min in 4 °C, followed by using BD Cytotfix/Cytoperm buffer (BD Biosciences, U.S.A) to fix and permeabilize cells. Next, cells were stained with BV421 anti-human IL-17A, PE-conjugated anti-human IFN- $\gamma$ , and PECY7 anti-human IL-4.

Isolated lymphocytes from the lung and colon were preincubated with anti-mouse CD16/32 to block Fc receptors and washed before staining. Surface antibodies in this experiment included FITC-conjugated anti-CD4, APC-CY7 anti-mouse CD3, and PercPCy5.5 conjugated anti-CD25. The 7-AAD staining was used to identify dead cells. For intracellular cytokine staining, cells were stimulated with Cell Stimulation Cocktail (eBioscience, U.S.A) and incubated for 5 h at 37°C, followed by using BD Cytotfix/Cytoperm buffer to fix and permeabilize cells. Cells were then stained with PE-conjugated IL-17A. For the detection of transcription factors, cells were fixed and permeabilized with the Foxp3/Transcription Factor Staining Buffer Set (eBioscience, U.S.A) according to the manufacturer's instructions and stained with the antibody APC-Foxp3. Cells were detected by FACSCantoTM (BD Biosciences, U.S.A) and analyzed by FlowJo software.

## DNA Extraction, 16S rRNA Gene Amplification and Sequencing, and Raw Data Analysis

Fecal DNA was extracted using the QIAamp DNA Stool Mini Kit (Qiagen Ltd., Germany) following the manufacturer's protocol. The V3-V4 region of the 16S rRNA gene was amplified using universal primers 338F (ACTCCTACGGGAGGCAGCAG) and 806R (GGACTACHVGGGTWTCTAAT). After purification and quantification, the PCR products were pooled into equimolar amounts and sequenced on the Illumina MiSeq sequencer to generate paired-end reads of 300 bp.

Raw FASTQ files were de-multiplexed and quality-filtered using QIIME (version 1.9). In brief, low-quality sequences with a length of < 220 nt or > 500 nt, an average quality score of < 20, and sequences containing > 3 nitrogenous bases were removed. The remaining high-quality reads were then clustered into operational taxonomic units

(OTUs) at a 97% similarity cutoff using UPARSE (version 7.1) and chimeric sequences were removed using UCHIME. Taxonomy assignment of OTUs was conducted using the RDP classifier against the SILVA 16S rRNA gene database (Release 132) with a confidence threshold of 0.70.

Alpha diversity was determined via sobs and Shannon indexes calculated by QIIME (version 1.9). Bar plots were obtained using the “vegan” package in R (version 3.3.1). Principal coordinates analysis (PCoA) was carried out based on Bray-Curtis and Jaccard distances using QIIME (version 1.9) to evaluate beta diversities. Besides, permutational multivariate analysis of variance (PERMANOVA, with 1,000 Monte Carlo permutations) was conducted based on the above distance matrices to compare the similarity of community structures between groups using the Adonis function available in the “vegan” package of R (version 3.3.1). The differentially abundant bacterial taxa among groups were identified using discriminant analysis (LDA) effect size (LEfSe) analysis. Only taxa with an average relative abundance greater than 0.01% were considered.

## Statistical Analysis

Data were analyzed using SPSS 22.0 (SPSS Inc., USA). All parametric data were analyzed using unpaired one-way ANOVA with Tukey’s post hoc test. All nonparametric data were analyzed using the Kruskal–Wallis test and *P* values for multiple comparisons were adjusted with a false discovery rate (FDR) according to Benjamini and Hochberg.<sup>40</sup> All corrected *P* values less than 0.05 were considered statistically significant. Data were expressed as means and standard error of the mean (SEM). Correlations between different bacterial taxa and inflammatory cytokines were evaluated using Spearman correlation analysis with the “pheatmap” package in R (version 3.3.1).

## Results

### COPD Patients Have a Higher Th17/Treg Ratio Than Healthy Subjects

Since inflammatory cells, especially T cells, play an important role in the progress of COPD, we enrolled a total of 25 subjects including 15 COPD patients and 10 healthy subjects to determine the difference of Th17 and Treg cells between the two groups. Baseline characteristics of COPD and healthy subjects are summarized in Table 2. Compared with healthy controls, these COPD clinical

patients showed a higher level of Th17 cells ( $P < 0.01$ , Figure 2A and C) but a lower proportion of Treg cells ( $P < 0.01$ , Figure 2B and D) in the PBMCs than healthy controls. In terms of the Th17/Treg ratio, it showed a significant increase in the COPD group in comparison with healthy subjects ( $P < 0.001$ , Figure 2E). These results suggested the important role of the Th17/Treg imbalance during the COPD exacerbations, which contributes to further exploration of the drug therapy for lung inflammation by modulating these two cell subtypes and other factors using a murine model suffering from COPD.

### XBCQ Administration Reduces the Weight Loss of COPD Mice

XBCQ is a representative Chinese medicine prescription and has a powerful adjunctive efficacy in alleviating clinical COPD.<sup>25</sup> Therefore, we subsequently explored the efficacy of XBCQ attenuating the exacerbation of COPD using an experimental mouse model induced by CSE combining with LPS. Firstly, we parsed predominant chemical constituents in XBCQ using the HPLC fingerprint. As shown in Figure 3, seven major compounds were identified including amygdalin, rutin, isoquercitrin, aloemodin, rhein, emodin, and chrysophanol.

Compared with the control, the stimulation of LPS and CSE significantly and persistently decreased the body weight of mice from day 15 of modeling (Figure 4A,  $P < 0.05$ ). However, the weight loss of COPD mice was effectively reduced after the introduction of L-XBCQ and M-XBCQ treatments, and the change of the latter was more obvious ( $P < 0.05$ , Figure 4A). Interestingly, the usage of DEX further aggravated the weight loss in the COPD group ( $P < 0.05$ , Figure 4A). No significant changes were observed in the H-XBCQ treatment ( $P > 0.05$ , Figure 4A). Therefore, the M-XBCQ treatment was more beneficial to reduce the weight loss of CSE and LPS-induced COPD mice relative to other groups.

### XBCQ Administration Improves the Lung Function of COPD Mice

We subsequently determined the changes in the pulmonary function of COPD mice. Compared with the untreated COPD group, FEV0.2/FVC was remarkably increased in COPD mice receiving M-XBCQ and DEX administration ( $P < 0.05$ , Figure 4B), indicating the mitigation of airway inflammation of these two groups. Besides, the H&E staining of lung tissue sections showed an inflammatory cell

**Table 2** Baseline Characteristics of Participants

Characteristic	Control	COPD
Number (male/female)	10 (2/8)	15 (12/3)
Age	47.20 ± 4.49	73.20 ± 2.12
Body mass index (kg/m <sup>2</sup> )	21.44 ± 1.17	26.40 ± 1.17
Smoking history	0	12
Smoking index (SI)		
SI = 0	10	3
400 ≤ SI ≤ 500	N/A	3
800 ≤ SI ≤ 900	N/A	5
1,000 ≤ SI	N/A	4
Comorbidities		
Allergic rhinitis	0	2
Blood routine examination (10 <sup>9</sup> /L)		
Leukocytes	5.48 ± 0.36	6.38 ± 0.34
Neutrophils	3.52 ± 0.26	4.19 ± 0.32
Eosinophils	0.20 ± 0.07	0.18 ± 0.03
Pulmonary function		
FEV1 (%)	N/A	72.30 ± 3.38
FEV1/FVC (%)	N/A	68.86 ± 2.55

**Note:** Smoking index, cigarettes smoked per day × years of smoking.

infiltrate around the bronchus, thickened mucosal epithelium, and alveolar enlargement in the non-treated COPD group (Figure 4C). However, M-XBCQ and H-XBCQ therapies significantly ameliorated these adverse alterations and the changes of the DEX treatment were similar to the M-XBCQ treatment (Figure 4C). No significant change was appeared in the L-XBCQ group (Figure 4C). These outcomes suggested that XBCQ treatments, especially M-XBCQ, improved the lung function of CSE and LPS-induced COPD mice. Based on these above results, we chose the middle dose of XBCQ as the best treatment dosage for subsequent exploration.

### XBCQ Administration Alleviates the Pulmonary Inflammation of COPD Mice

Next, we measured the mRNA expression of proinflammatory biomarkers in lung tissues using qPCR to evaluate the inflammatory responses of mice. The mRNA expressions of TNF- $\alpha$  and IL-1 $\beta$  were extremely up-regulated in the lung tissues of COPD mice while M-XBCQ and DEX treatments significantly suppressed these increases ( $P < 0.05$ , Figure 5A). Similarly, the IHC assay demonstrated that the protein expression of MMP-9, which mediates the

process of pulmonary inflammation, was significantly higher in the lung tissues of COPD mice than that of the control ( $P < 0.01$ , Figure 5B and C). On the contrary, M-XBCQ treatment also significantly inhibited this up-regulation ( $P < 0.05$ , Figure 5B and C). These findings indicated that XBCQ and DEX contributed to alleviating the pulmonary inflammatory responses in COPD mice.

### XBCQ Administration Inhibits the Th17/Treg Imbalance in the Lung and Colon of COPD Mice

We then performed the flow cytometry analysis to detect the distribution of Th17 and Treg cells in the lung and colon of COPD mice. As shown in Figure 6, compared with the control, IL-17A<sup>+</sup>Th17 cells were significantly enriched but the proportion of Foxp3<sup>+</sup>Treg cells were remarkably decreased in the lung and colon of the COPD group (Figure 6A and B). Thus, COPD mice showed higher Th17/Treg ratios were presented in both the lung and colon ( $P < 0.05$ , Figure 6C). As expected, M-XBCQ treatments distinctly recovered the balance of Th17 and Treg cells in COPD mice ( $P < 0.05$ , Figure 6C) by inhibiting the accumulation of Th17 cells and rectifying the deficiency of Treg cells (Figure 6A and B). These data suggested that M-XBCQ administration served as an effective damper on the Th17/Treg imbalance in the lung and colon of COPD mice.

### XBCQ Administration Alleviates the Gut Dysbiosis of COPD Mice

Since the gut microbiota plays a key role in the progression of COPD, we further examined the effects of XBCQ intervention on gut microbiota composition in experimental COPD mice. A total of 749,170 high-quality sequences were generated with an average of 62,430 reads in each sample. Subsequently, we randomly rarefied each sample to 27,617 reads for downstream analysis to minimize the impacts of sequencing depth. Based on 97% sequence similarity, these remaining reads were clustered and classified into 9 phyla, 17 classes, 23 orders, 33 families, and 86 genera.

At the community level, we observed that COPD mice had a remarkably lower sobs index in the colonic microbiota than controls ( $P < 0.05$ , Figure 7A), indicating a lower microbial richness. However, the M-XBCQ administration induced an increasing trend in the sobs index of this group ( $P < 0.10$ , Figure 7A). The overall



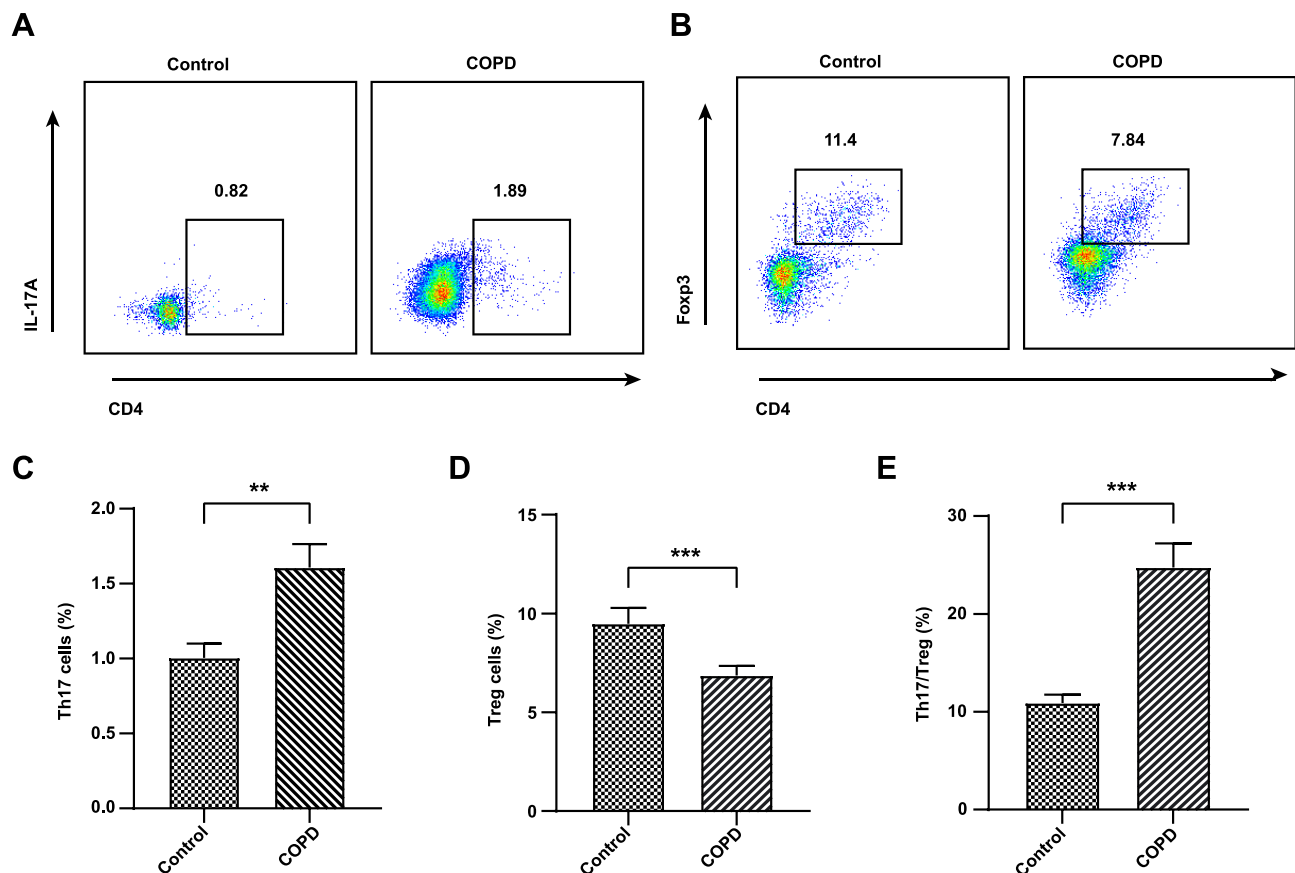


**Figure 2** Flow cytometry of Th17 and Treg cells in the serum of COPD patients and healthy subjects. The representative plots of Th17 cells gated by  $CD3^+CD4^+IL17^+$  (A). The representative plots of Treg cells gated by  $CD3^+CD4^+CD25^+Foxp3^+$  (B). The level of Th17 cells (C). The level of Treg cells (D). The Th17/Treg ratio (E). Data were expressed as mean  $\pm$  SEM. \*\*\* $P < 0.001$ , \*\* $P < 0.01$ , compared with healthy controls.

composition of the colonic microbiota was significantly different among the three groups (Figure 7B–D). PCoA plots based upon Bray-Curtis distances and Jaccard distances further confirmed the dramatic separation of colonic samples among different groups (Figure 7E). PERMANOVA based on these distances also showed that the microbiota structures were strongly influenced by CSE and XBCQ administration (Bray-Curtis distance,  $R^2 = 0.485$ ,  $P = 0.001$ ; Jaccard distances,  $R^2 = 0.405$ ,  $P = 0.001$ ).

Next, we performed the LefSe analysis to identify differentially abundant microbes contributing to the distinction among three groups of mice. As indicated in Figure 8A and B, four genera were enriched in the colon of COPD mice but 15 genera presented lower abundances than the control group. Of note, *Gordonibacter*, *Allobaculum*, *Tyzzera\_3*, *Akkermansia*, and *Subdoligranulum* were less abundant in COPD mice than controls, whereas they were significantly enriched upon the M-XBCQ administration. Besides, compared with the control group, *Bifidobacteria*, *Roseburia*,

*Helicobacter*, *Prevotellaceae\_Ga6A1\_group*, *Staphylococcus*, *Ruminiclostridium\_5*, *Coprococcus\_1*, and *Faecalibaculum* were also less abundant in COPD mice. On the contrary, *Streptococcus*, *Marvinbryantia*, *Candidatus\_Stoquefichus*, and *Coriobacteriaceae\_UCG-002* exhibited higher relative proportions in the colon of COPD mice compared to the control group. However, the M-XBCQ treatment remarkably inhibited the accumulation of *Streptococcus* and *Marvinbryantia*. These results showed an imbalanced state of the gut microbiota in COPD mice and the M-XBCQ administration had the potential to ameliorate this gut dysbiosis to a certain extent.

### Specific Microbes Affected by XBCQ are Significantly Correlated to the Lung Inflammation

A Spearman correlation matrix was generated to determine the associations between the bacterial genera and inflammatory parameters that were dramatically affected by

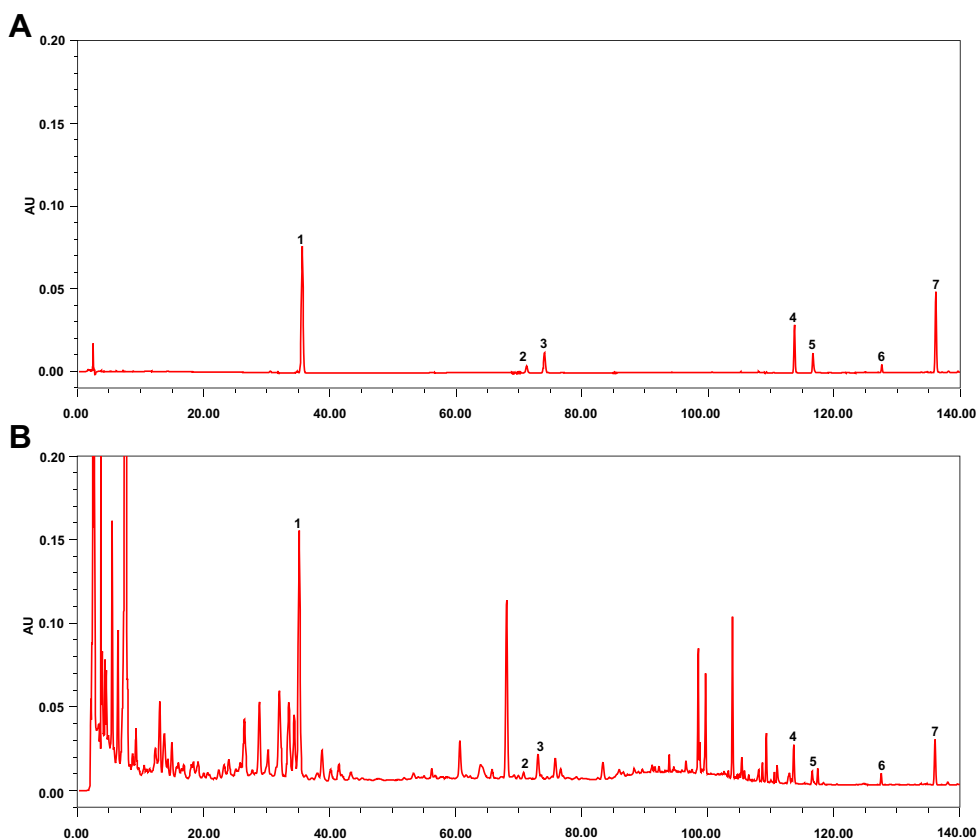


**Figure 3** Major chemical compounds in XBCQ by HPLC analysis. Mixed standard substances (A). XBCQ sample, peaks 1, 2, 3, 4, 5, 6, and 7 are derived from amygdalin, rutin, isoquercitrin, aloee-emodin, rhein, emodin, and chrysophanol, respectively (B).

experimental COPD. As suggested in Figure 9, significant correlations were identified between gut microbiota and lung inflammatory responses. In particular, several genera having lower abundances in COPD mice, including *Allobaculum*, *Tyzzereia\_3*, *Prevotellaceae\_Ga6A1\_group*, *Helicobacter*, *Faecalibaculum*, and *Subdoligranulum*, were positively correlated to body weight and lung function, but negatively associated with the Th17/Treg ratio and proinflammatory cytokines in the lung. Additionally, *Gordonibacter* and *Akkermansia* showed similar significant trends to correlate with the above parameters. By contrast, *Candidatus\_Stoquefichus*, *Streptococcus*, and *Marvinbryantia*, enriched in COPD mice, presented strongly negative association coefficients with body weight and lung function but positive correlations to the Th17/Treg balance and proinflammatory cytokines. Therefore, the changes in the lung inflammatory status of COPD mice might be partly modulated by their intestinal microbiota.

## Discussion

COPD is a clinically representative obstructive airway disease and has become the third most common cause of death worldwide.<sup>1,2</sup> As a consequence, it is urgent to disclose the pathogenesis of COPD and explore novel prevention and treatment. XBCQ is a traditional Chinese medicine prescription responsible for alleviating the clinical symptoms of patients with COPD.<sup>25</sup> On this basis, the present research mainly focused on the Th17/Treg imbalance and gut dysbiosis induced by COPD and investigated the efficacy and mechanisms of XBCQ treatment on the inflammatory process of COPD. To our knowledge, our findings show, for the first time, that the oral dosage of XBCQ, especially M-XBCQ, had protective effects against the lung inflammation caused by experimental COPD. This might be attributable to the maintenance of the Th17/Treg balance in the lung and colon and the improvement of their gut bacterial community by XBCQ administration.

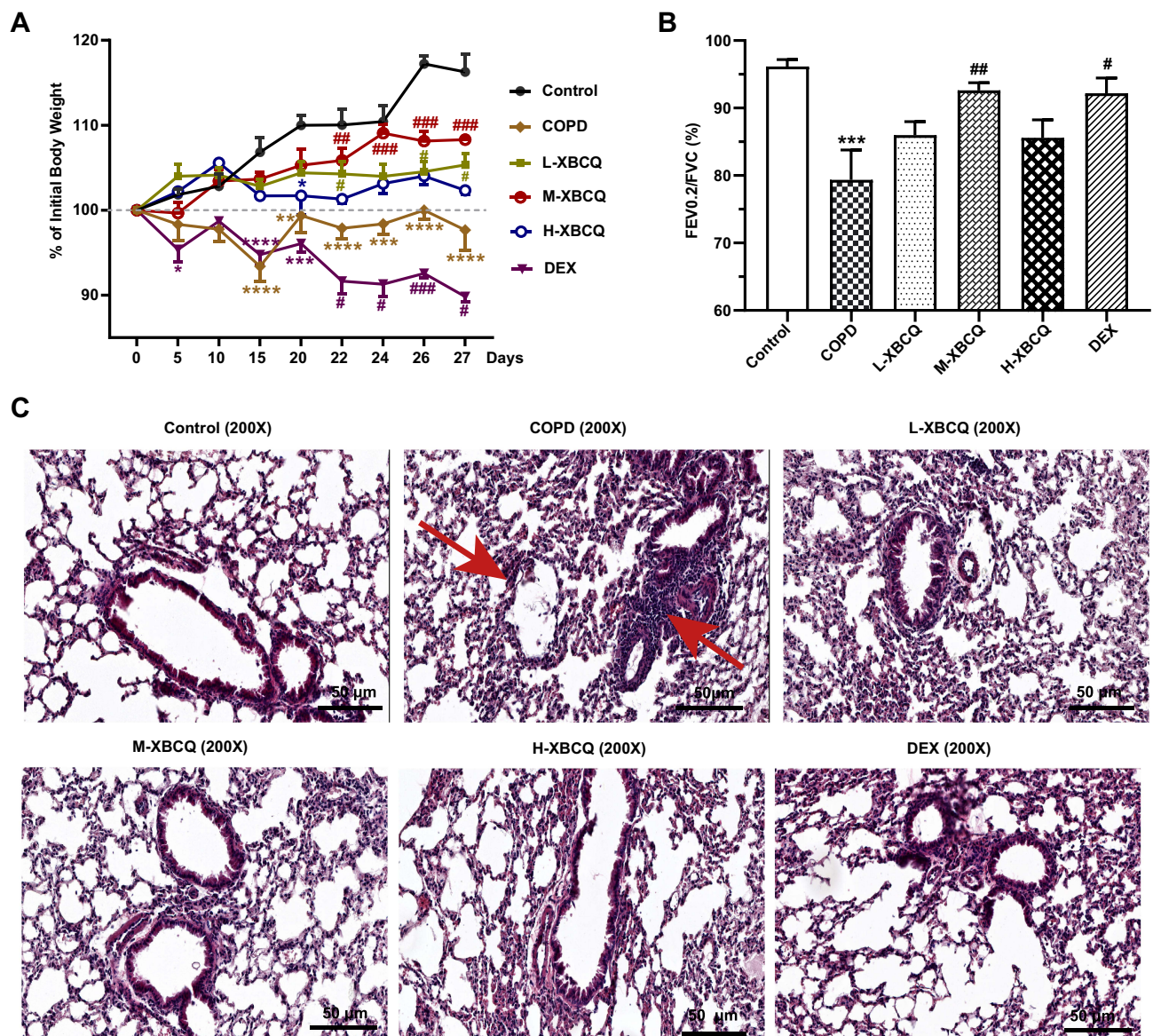


**Figure 4** Effects of XBCQ treatment on body weight and lung function in CSE and LPS-induced COPD mice. Body weight changes throughout the entire duration of this study, in which mice were weighed every 5 days before administration and every 2 days after administration (A). The ratio of FEV0.2/FVC (B). Lung pathological slides by the H&E staining, where the red arrows indicate the alveolar septum rupture and the infiltration of periracheal inflammatory cells (C). Data were expressed as mean  $\pm$  SEM. \*\*\*\* $p < 0.0001$ , \*\*\* $p < 0.001$ , \*\* $p < 0.01$ , \* $p < 0.05$ , compared with the control group. #### $p < 0.001$ , ### $p < 0.01$ , # $p < 0.05$ , compared with the COPD group.

**Abbreviations:** L-XBCQ, the low dose of XBCQ; M-XBCQ, the middle dose of XBCQ; H-XBCQ, the high dose of XBCQ; DEX, dexamethasone.

The homeostasis between Th17 and Treg cells has emerged as a highlighted factor in maintaining health and exacerbating autoimmunity.<sup>41</sup> Th17 cells are an important subset of effector T cells and excessive Th17 responses are also correlated to various pathogenic states dependent on the production of pro-inflammatory cytokines including IL-17A.<sup>42</sup> Treg cells, generally defined as CD4<sup>+</sup>CD25<sup>+</sup>Foxp3<sup>+</sup> T cells, have been predominantly recognized for their ability to suppress inflammation by producing anti-inflammatory cytokines such as IL-10.<sup>42</sup> Numerous studies support the imbalance between these

two subsets leading to the development and progression of COPD.<sup>5-7,12</sup> In our clinical trial, we reported that these COPD volunteers exhibited more IL-17A-secreting Th17 cells but lower Foxp3<sup>+</sup> Treg cells in their serum compared with normal controls. As a consequence, higher Th17/Treg ratios were appeared in these COPD patients, reflecting an abnormal state between these two subtypes. In agreement with our findings, several previous researches have also proved that COPD patients exhibit more Th17-related cytokines but lower Treg cells and lower mRNA levels for Foxp3 than control subjects.<sup>8,10,11</sup> Herein, our



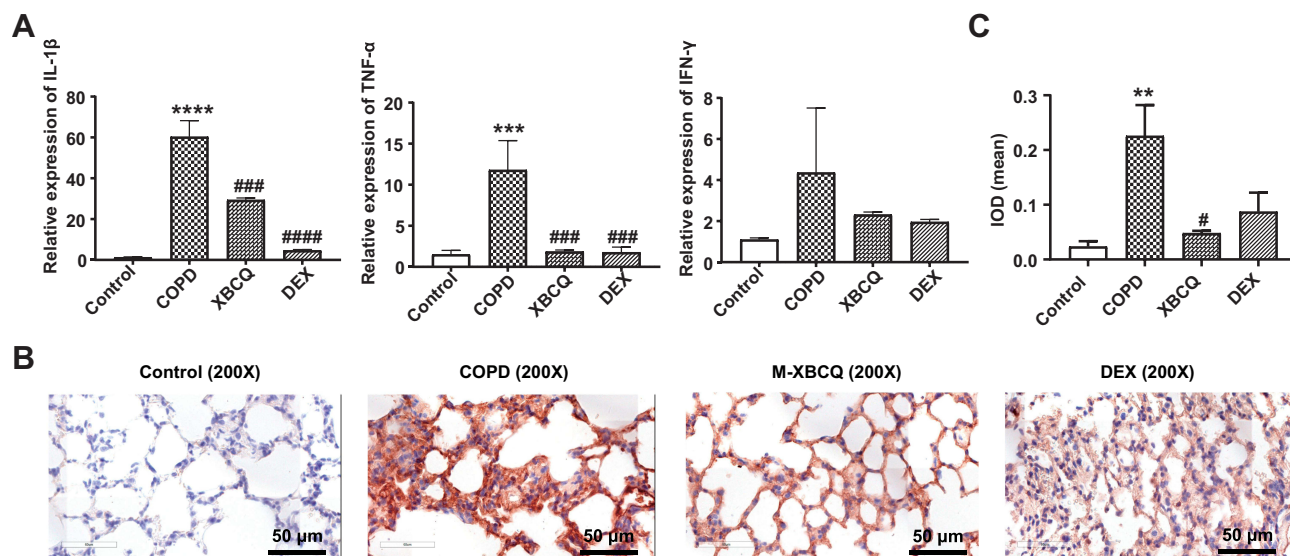


**Figure 5** Effects of the middle dose of XBCQ on the lung inflammation in COPD mice. The mRNA expressions of inflammatory cytokines including TNF- $\alpha$ , IL-1 $\beta$ , and IFN- $\gamma$  (A). The immunohistochemistry staining of MMP-9 in the lung tissue (B). The integrated optical density (IOD) of MMP-9 (C). Data are expressed as mean  $\pm$  SEM. \*\*\*\* $P$  < 0.0001, \*\*\* $P$  < 0.001, \*\* $P$  < 0.01, compared with the control group. #### $P$  < 0.0001, ### $P$  < 0.001, # $P$  < 0.05, compared with the COPD group.

**Abbreviations:** M-XBCQ, the middle dose of XBCQ; DEX, dexamethasone.

observations demonstrated again the vital role of the Th17/Treg imbalance in mediating the pathogenesis of COPD. The regulation of Th17/Treg balance, therefore, might be considered a crucial target for the treatment of COPD.

As a Chinese classical prescription, XBCQ has been widely reported to treat COPD via inhibiting excessive inflammatory responses and recovering lung function with few adverse drug reactions.<sup>24–27</sup> In the follow-up study, we established a mouse model with COPD by the intranasal inhalation of CSE and LPS,<sup>43</sup> to investigate the mechanisms by which XBCQ alleviates pulmonary inflammation. Most COPD patients have a loss of body weight related to COPD management.<sup>44</sup> In consistent with our clinical results, the animal trial suggested again that the higher ratio of Th17 cells to Treg cells has also appeared in the lung and colon of COPD mice. Surprisingly, M-XBCQ remarkably inhibited the accumulation of Th17 cells and the deficiency of Treg cells in both two kinds of tissues, resulting in a recovery of the balance between these two subsets. Herein, we demonstrated that the Th17/Treg balance acts as a crucial part of the treatment of lung inflammation by M-XBCQ administration.

Besides, we observed that CSE-treated mice with COPD presented an extremely lower body weight in comparison with the control group. However, the XBCQ administration, especially the middle dose of XBCQ (M-XBCQ) at a concentration of 0.7 g/mL, had a significant inhibitory effect on the weight loss of

COPD mice. As we know, the broken lung function with the low FEV1/FVC ratio, as the gold standard for the COPD diagnosis, is also involved in its exacerbation.<sup>45</sup> In agreement with clinical COPD, the experimental COPD mice in this study also exhibited the destroyed lung function as reflected by the lower proportion for FEV0.2 to FVC. As expected, the M-XBCQ treatment had a great potential to improve the lung function of COPD mice, which is similar to a previous research using a clinical trial.<sup>25</sup> These above outcomes reveal that M-XBCQ contributes more to the treatment of COPD by improving lung function and promoting the normalization of lung tissues.

Many previous studies have reported that several primary active ingredients in medicinal herbs comprising the XBCQ formula, such as rhein, emodin, and chrysophanol<sup>46–48</sup> in *Rheum officinale Baill*, calcium sulfate in *Gypsum Fibrosum*, rutin and amygdalin<sup>49,50</sup> in *Prunus armeniaca L.*, and isoquercitrin<sup>51</sup> in *Trichosanthes kirilowii Maxim*, are equipped with distinct anti-inflammatory activities. On this account, in this study, the expanded inflammatory cell infiltrations in the lung tissues of COPD mice, one of the major pathologic features from COPD patients,<sup>52</sup> were significantly suppressed by XBCQ treatments. On the other hand, a variety of pro-inflammatory cytokines, such as TNF- $\alpha$  and IL-1 $\beta$ , generally exhibits much higher levels in both sputum and serum during COPD exacerbations,<sup>25,53</sup> which are similar to our



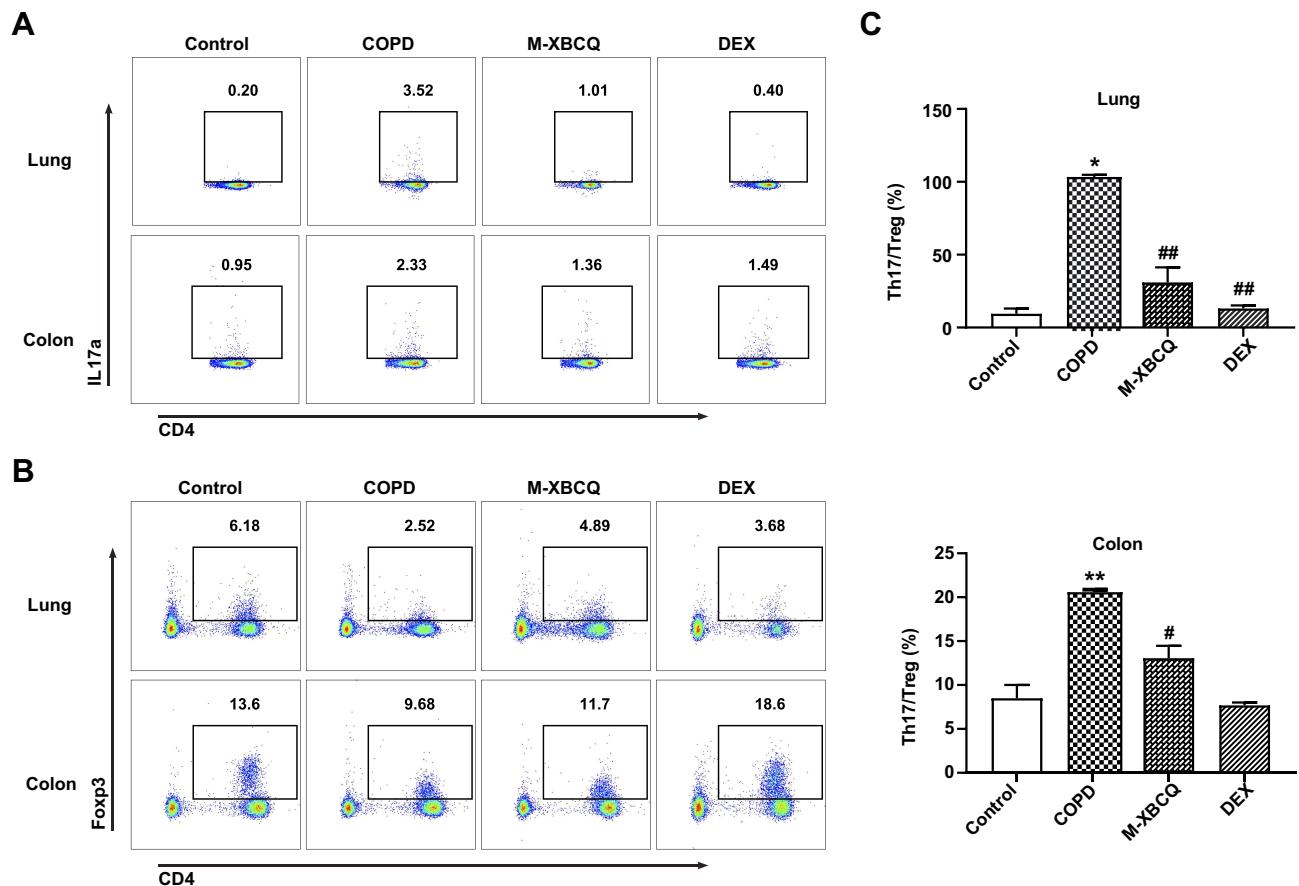


**Figure 6** Flow cytometry of Th17 and Treg cells in the lung and colon of COPD mice. The representative plots of Th17 cells gated by  $CD3^+CD4^+IL17^+$  (A). The representative plots of Treg cells gated by  $CD3^+CD4^+CD25^+Foxp3^+$  (B). The Th17/Treg ratio in lung and colon (C). Data are expressed as mean  $\pm$  SEM. \*\* $P < 0.01$ , \* $P < 0.05$ , compared with control group. ## $P < 0.01$ , # $P < 0.05$ , compared with COPD group.

**Abbreviations:** M-XBCQ, the middle dose of XBCQ; DEX, dexamethasone.

results in the lung tissues of COPD mice. Not unexpectedly, the concentrations of these above pro-inflammatory mediators in the M-XBCQ group were significantly lower than those in the model group.

As well, matrix metalloproteinases including MMP-9 are a group of zinc-dependent endopeptidases that uniquely mediates lung inflammation through remodeling extracellular matrix turnover and activating of nonmatrix substrates including cytokines.<sup>54</sup> Normal lungs do not contain MMP-9, but there is an increase of MMP-9 transcription and expression under inflammatory conditions due to cell infiltration such as neutrophils. During the progress of COPD, bronchial epithelial cells and leukocytes can produce MMP-9 in the lung.<sup>55,56</sup> Another research has also identified that MMP-9 could be regarded as a biomarker for the severity of COPD.<sup>57</sup> Our results also showed that the expression of MMP-9 was remarkably enhanced in the lung tissues of COPD mice. However, the M-XBCQ treatment significantly inhibited

the expression of MMP-9. We speculated that these observed alterations might partly explain the improvement of the damages in alveolar walls and lung inflammatory cell infiltrates derived from COPD mice by the XBCQ administration. It is worth noting that the common dexamethasone treatment also improved lung function and alleviated lung inflammatory status. Nonetheless, compared with the XBCQ administration, this management had no inhibitory impact on the MMP-9 expression in lung tissues and the Th17/Treg imbalance in the colon, as well as led to further weight loss. This implicated the adverse reactions of dexamethasone to some extent, which remains to be further studied. Based on these outcomes, we propose that M-XBCQ, as an adjuvant treatment, is conducive to alleviating the respiratory inflammatory responses during the process of COPD.

Apart from inflammatory cells and cytokines, the alterations in microbial composition and function in the respiratory tract and the intestine appear to be typical

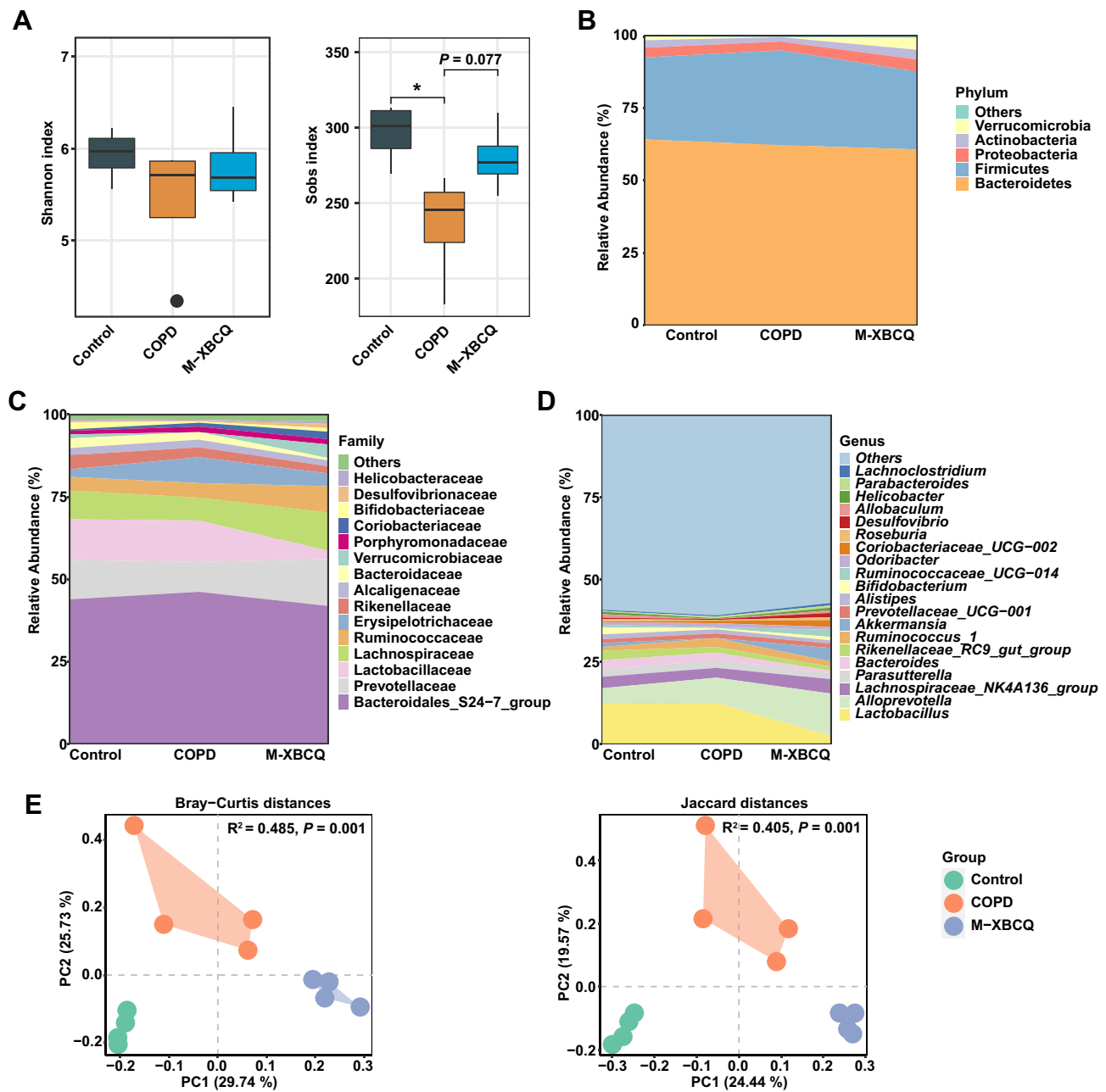


**Figure 7** The alterations in the colonic microbiota structure of COPD mice. Shannon and sobs index (A). Abundant phyla (B), families (C), and genera (D) in the colonic microbiota of mice. Principal coordinate analysis (PCoA) based on Bray-Curtis and Jaccard distances (E).

**Abbreviations:** M-XBCQ, the middle dose of XBCQ. \* $P < 0.05$ , compared with control group.

gatekeepers resistant to the adherence by respiratory pathogens based on the “gut-lung axis”.<sup>19,58,59</sup> Bowerman et al have found that the gut microbiome and metabolome of COPD patients are significantly distinguished from healthy subjects,<sup>4</sup> which are similar to the observation in cigarette smoking-treated murine models with COPD.<sup>20,21</sup> In our study, we also identified the distinction of the colonic microbiome between healthy and

COPD mice. As well, the colon of CSE-induced COPD mice harbored less abundant *Gordonibacter* and *Allobaculum* compared with normal controls. *Gordonibacter*, which was declined in long-term smokers with Crohn’s disease and DSS-induced colitis mice, is correlated to metabolize dietary polyphenols.<sup>60–62</sup> *Allobaculum* has been associated previously with human diseases such as enteritis, insulin resistance, and adipose

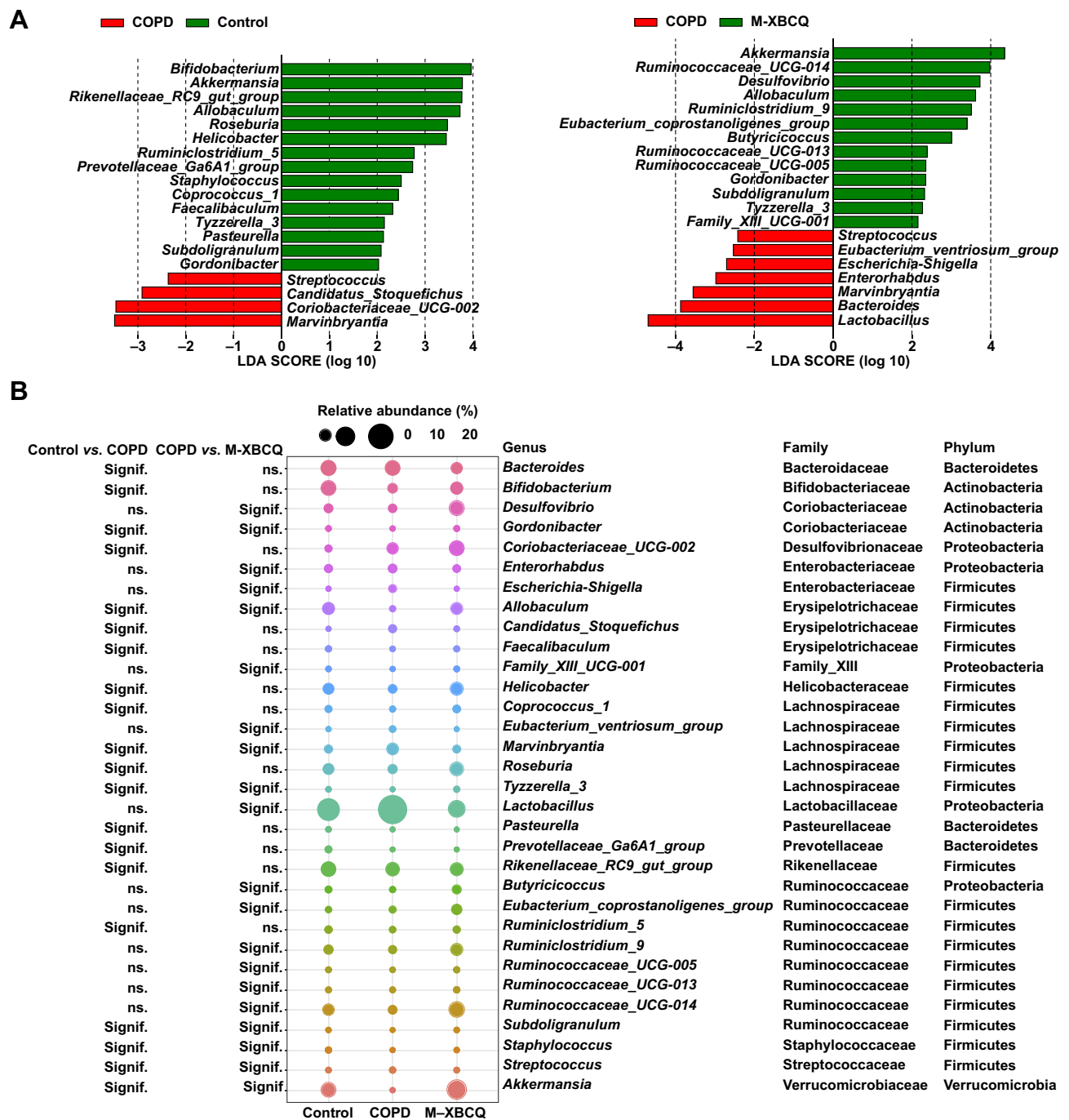


**Figure 8** Differentially abundant microbes among different groups. Differentially abundant genera identified by LEfSe with a linear discriminant analysis (LDA) score (threshold  $\geq 2$ ) (A). The bubble matrix shows the average relative abundances of these genera (B).

**Abbreviation:** M-XBCQ, the middle dose of XBCQ.

inflammation.<sup>63,64</sup> Additionally, the proportions of *Tyzzereella\_3* within Lachnospiraceae and *Subdoligranulum* within Ruminococcaceae were also decreased in COPD mice. Inhabitants belonging to these families were generally considered to be able to digest refractory carbohydrates to generate short-chain fatty acids,<sup>65</sup> which can maintain barrier function, reduce

inflammation in the intestine, and govern the Th17/Treg balance.<sup>66</sup> *Akkermansia muciniphila*, the main member from *Akkermansia spp.*, is a mucin-degrading organism, which has attracted increasing attention for its prominent health-promoting effects. Moreover, *A. muciniphila* has been previously associated with the production of T cell subtypes including Th17 and Treg cells, and therefore

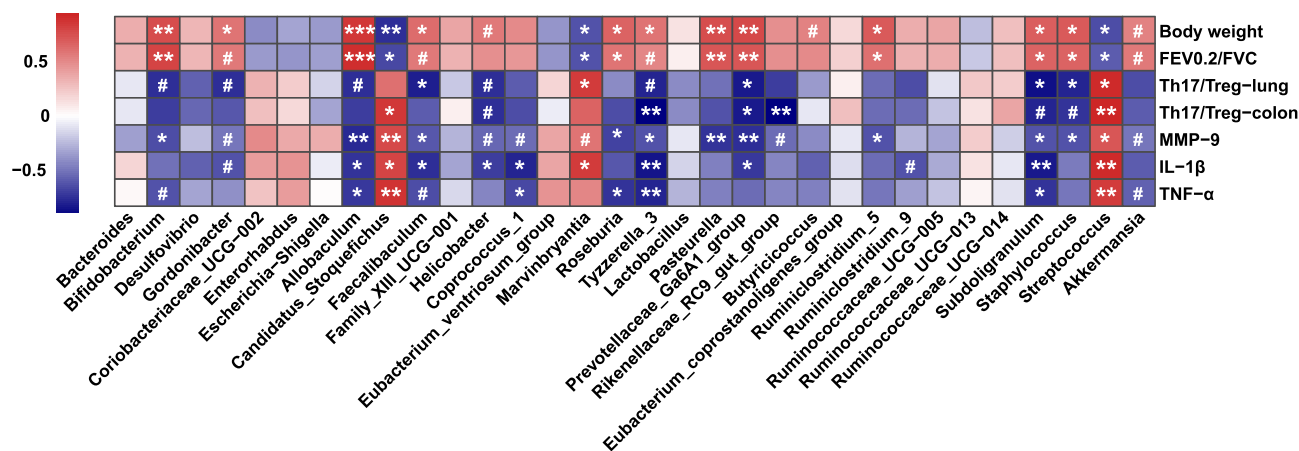


**Figure 9** Spearman correlation analysis between key genera and physiological parameters affected by experimental COPD. Cells are colored based on the Spearman correlation coefficient. The red indicates a positive correlation, and the blue indicates a negative correlation. Asterisks indicate statistically significant correlations, and hash signs indicate a significant correlation trend. \*\*\* $P < 0.001$ , \*\* $P < 0.01$ , \* $P < 0.05$ , # $P < 0.10$ .

effectively protects against airway inflammation.<sup>67,68</sup> In this study, *Akkermansia* spp. was significantly reduced in CSE-induced COPD, suggesting its pivotal role in mediating anti-inflammatory effects within the lung. However, the M-XBCQ administration caused strong enrichments of these above-mentioned microorganisms in COPD mice. On the contrary, we found that M-XBCQ strongly inhibited the excessive growth of the genera *Streptococcus* that was enriched in COPD mice. In line with us, the increased abundance of *Streptococcus* has also been widely observed in the gut and lung of COPD patients,<sup>4,18,69</sup> which might be as an adverse character during the COPD exacerbations. Altogether, our study is the first to highlight the protection of XBCQ against experimental COPD might be attributable to its beneficial effects on the intestinal microbiota.

On the other hand, along with the interaction between gut microbiota and host immunity, we further assessed the associations between microbes and inflammatory biomarkers impacted by XBCQ. Interestingly enough, we observed that *Gordonibacter*, *Allobaculum*, *Tyzzereia\_3*, *Subdoligranulum*, and *Akkermansia* presented significant positive associations with body weight and lung function, but negative correlations with the Th17/Treg ratio and proinflammatory cytokines. Opposite results were seen in the relevance between *Streptococcus* and physiological parameters. These outcomes reinforced that there might be a close relationship between pulmonary immune mechanisms and the microbes that colonize the intestine.

In our follow-up research, the germ-free or antibiotic-treated animal models combined with the microbiota

transplantation were urgently needed to further confirm the close interaction between Th17/Treg balance and gut microbiota. On the other hand, suppressing the polarization of Th17 cells would be another ideal manner to validate its mechanism mediating the curative effect of XBCQ on COPD. As well, the movement of metabolites derived from XBCQ-associated specific microbes along the “gut-lung axis” might be its underlying mechanism alleviating the pulmonary inflammation of COPD subjects by the XBCQ medication. Significantly, XBCQ, as a classical prescription for the treatment of COPD, is still an unknown “black box” composed of extremely complex chemical substances, which increases the necessity to understand the pharmacodynamic material basis. Further studies should also focus on the extraction and screening of key active compounds, followed by the verification tests in vivo and in vitro.

In terms of COPD modeling, we chose mice commonly used in many previous studies to establish experimental COPD models owing to their faster reproduction cycles, smaller sizes and easy to experiment, and better-studied genome sequences. However, mice lack a better similarity with human beings in the aspect of respiratory anatomies, such as the absence of goblet cells in the bronchi.<sup>70</sup> Besides, reliable evidence has shown that a significant difference in the damage degree existed between BALB/cJ and C57BL/6J mice when exposed to COPD stimulus, indicating the instability of the replication of COPD among different mouse strains.<sup>71</sup> In our study, we also observed that the body weight of COPD mice was fluctuated greatly during modeling before the XBCQ



administration, suggesting that the ideal modeling cycle for mice might be much longer. In this case, we propose that the subsequent study in the future could attempt to develop other more human-like models with COPD, such as guinea pigs.

## Conclusion

Taken together, our work suggests that clinical patients with COPD exhibit a systematically imbalanced state between Th17 and Treg cells relative to healthy controls. The middle dose of XBCQ (0.7 g/mL) causes a significant recovery of pulmonary function and inhibits the inflammatory infiltration in an experimental COPD murine model, which might be mediated via restoring the Th17/Treg homeostasis and rectifying the gut dysbiosis. Meanwhile, the alterations of lung inflammatory status might be partly modulated by the intestinal microbiota as the significant associations exist between specific bacterial genera (eg *Akkermansia* and *Streptococcus*, etc) and inflammatory biomarkers (eg Th17/Treg, IL-1 $\beta$ , and MMP-9, etc) affected by XBCQ. Collectively, our investigation provides novel insights for elucidating the mechanism by which XBCQ as a therapy for COPD in a microbiota-dependent manner via the gut-lung axis. Future studies will focus on identifying the main active components in XBCQ decoction and uncover specific microbial biomarkers and their derived metabolites affecting the immune responses in the process of COPD.

## Abbreviations

COPD, chronic obstructive pulmonary disease; CSE, cigarette smoke extract; GIT, gastrointestinal tract; XBCQ, Xuanbai Chengqi decoction; GOLD, Global Initiative for Chronic Obstructive Lung Disease; HPLC, high-performance liquid chromatography; L-XBCQ, low dose of XBCQ; M-XBCQ, middle dose of XBCQ; H-XBCQ, high dose of XBCQ; DEX, dexamethasone; H&E, hematoxylin and eosin; IHC, immunohistochemistry; MMP-9, matrix metalloproteinases-9; IOD, integral optical density; OTUs, operational taxonomic units; PCoA, principal coordinates analysis; PERMANOVA, permutational multivariate analysis of variance; LEfSe, discriminant analysis (LDA) effect size; FDR, false discovery rate; SEM, standard error of the mean.

## Data Sharing Statement

The raw sequencing data supporting this study are available in the NCBI Sequence Read Archive (SRA) repository under accession number SRP331895. The remaining

data that support the findings of this study are available from the corresponding author (Guiying Peng) upon reasonable request.

## Acknowledgments

This research was supported by the National Natural Science Foundation of China (Grant No. 81473656) and Fundamental Research Funds for Central Universities (Grant No. 2019-JYB-TD014). We sincerely thank Dr. Steven L. Brody from Washington University in St. Louis for reviewing the manuscript for language and technical content.

## Author Contributions

All authors made a significant contribution to the work reported, whether that is in the conception, study design, execution, acquisition of data, analysis and interpretation, or in all these areas; took part in drafting, revising or critically reviewing the article; gave final approval of the version to be published; have agreed on the journal to which the article has been submitted; and agree to be accountable for all aspects of the work.

## Disclosure

The authors report no conflicts of interest in this work.

## References

1. Guan WJ, Zheng XY, Chung KF, Zhong NS. Impact of air pollution on the burden of chronic respiratory diseases in China: time for urgent action. *Lancet*. 2016;388(10054):1939–1951. doi:10.1016/S0140-6736(16)31597-5
2. Collaborators GBDCoD. Global, regional, and national age-sex specific mortality for 264 causes of death, 1980–2016: a systematic analysis for the Global Burden of Disease Study 2016. *Lancet*. 2017;390(10100):1151–1210. doi:10.1016/S0140-6736(17)32152-9
3. Barnes PJ. Targeting cytokines to treat asthma and chronic obstructive pulmonary disease. *Nat Rev Immunol*. 2018;18(7):454–466. doi:10.1038/s41577-018-0006-6
4. Bowerman KL, Rehman SF, Vaughan A, et al. Disease-associated gut microbiome and metabolome changes in patients with chronic obstructive pulmonary disease. *Nat Commun*. 2020;11(1):5886. doi:10.1038/s41467-020-19701-0
5. Zheng X, Zhang L, Chen J, Gu Y, Xu J, Ouyang Y. Dendritic cells and Th17/Treg ratio play critical roles in pathogenic process of chronic obstructive pulmonary disease. *Biomed Pharmacother*. 2018;108:1141–1151. doi:10.1016/j.biopha.2018.09.113
6. Alcorn JF, Crowe CR, Kolls JK. TH17 cells in asthma and COPD. *Annu Rev Physiol*. 2010;72:495–516. doi:10.1146/annurev-physiol-021909-135926
7. Weaver CT, Hatton RD. Interplay between the TH17 and TReg cell lineages: a (co-) evolutionary perspective. *Nat Rev Immunol*. 2009;9(12):883–889. doi:10.1038/nri2660
8. Di Stefano A, Caramori G, Gnemmi I, et al. T helper type 17-related cytokine expression is increased in the bronchial mucosa of stable chronic obstructive pulmonary disease patients. *Clin Exp Immunol*. 2009;157(2):316–324. doi:10.1111/j.1365-2249.2009.03965.x

9. Brusselle GG, Joos GF, Bracke KR. New insights into the immunology of chronic obstructive pulmonary disease. *Lancet*. 2011;378(9795):1015–1026. doi:10.1016/S0140-6736(11)60988-4
10. Lee SH, Goswami S, Grudo A, et al. Antielastin autoimmunity in tobacco smoking-induced emphysema. *Nat Med*. 2007;13(5):567–569. doi:10.1038/nm1583
11. Hou J, Sun Y, Hao Y, et al. Imbalance between subpopulations of regulatory T cells in COPD. *Thorax*. 2013;68(12):1131–1139. doi:10.1136/thoraxjnl-2012-201956
12. Cervilha DAB, Ito JT, Lourenço JD, et al. The th17/treg cytokine imbalance in chronic obstructive pulmonary disease exacerbation in an animal model of cigarette smoke exposure and lipopolysaccharide challenge association. *Sci Rep*. 2019;9(1):1921. doi:10.1038/s41598-019-38600-z
13. Donaldson GP, Lee SM, Mazmanian SK. Gut biogeography of the bacterial microbiota. *Nat Rev Microbiol*. 2016;14(1):20–32. doi:10.1038/nrmicro3552
14. Li N, Zuo B, Huang S, et al. Spatial heterogeneity of bacterial colonization across different gut segments following inter-species microbiota transplantation. *Microbiome*. 2020;8(1):161. doi:10.1186/s40168-020-00917-7
15. Mendez R, Banerjee S, Bhattacharya SK, Banerjee S. Lung inflammation and disease: a perspective on microbial homeostasis and metabolism. *IUBMB Life*. 2019;71(2):152–165. doi:10.1002/iub.1969
16. Caballero S, Pamer EG. Microbiota-mediated inflammation and antimicrobial defense in the intestine. *Annu Rev Immunol*. 2015;33:227–256. doi:10.1146/annurev-immunol-032713-120238
17. Mayhew D, Devos N, Lambert C, et al. Longitudinal profiling of the lung microbiome in the AERIS study demonstrates repeatability of bacterial and eosinophilic COPD exacerbations. *Thorax*. 2018;73(5):422–430. doi:10.1136/thoraxjnl-2017-210408
18. Pragman AA, Lyu T, Baller JA, et al. The lung tissue microbiota of mild and moderate chronic obstructive pulmonary disease. *Microbiome*. 2018;6(1):7. doi:10.1186/s40168-017-0381-4
19. He Y, Wen Q, Yao F, Xu D, Huang Y, Wang J. Gut-lung axis: the microbial contributions and clinical implications. *Crit Rev Microbiol*. 2017;43(1):81–95. doi:10.1080/1040841X.2016.1176988
20. Allais L, Kerckhof FM, Verschuere S, et al. Chronic cigarette smoke exposure induces microbial and inflammatory shifts and mucin changes in the murine gut. *Environ Microbiol*. 2016;18(5):1352–1363. doi:10.1111/1462-2920.12934
21. Lai HC, Lin TL, Chen TW, et al. Gut microbiota modulates COPD pathogenesis: role of anti-inflammatory *Parabacteroides goldsteinii* lipopolysaccharide. *Gut*. 2021;gutjnl-2020-322599. doi:10.1136/gutjnl-2020-322599
22. Pandiyan P, Bhaskaran N, Zou M, Schneider E, Jayaraman S, Huehn J. Microbiome dependent regulation of Tregs and Th17 cells in mucosa. *Front Immunol*. 2019;10:426. doi:10.3389/fimmu.2019.00426
23. Omenetti S, Pizarro TT. The Treg/Th17 axis: a dynamic balance regulated by the gut microbiome. *Front Immunol*. 2015;6:639. doi:10.3389/fimmu.2015.00639
24. Jin J, Zhang H, Li D, et al. Effectiveness of Xin Jia Xuan Bai Cheng Qi Decoction in treating acute exacerbation of chronic obstructive pulmonary disease: study protocol for a multicentre, randomised, controlled trial. *BMJ Open*. 2019;9(11):e030249. doi:10.1136/bmjopen-2019-030249
25. Liu M, Zhong X, Li Y, et al. Xuan Bai Cheng Qi formula as an adjuvant treatment of acute exacerbation of chronic obstructive pulmonary disease of the syndrome type phlegm-heat obstructing the lungs: a multicenter, randomized, double-blind, placebo-controlled clinical trial. *BMC Complement Altern Med*. 2014;14(1):239. doi:10.1186/1472-6882-14-239
26. Qin H, Wen HT, Gu KJ, et al. Total extract of Xin Jia Xuan Bai Cheng Qi decoction inhibits pulmonary fibrosis via the TGF-beta/Smad signaling pathways in vivo and in vitro. *Drug Des Devel Ther*. 2019;13:2873–2886. doi:10.2147/DDDT.S185418
27. Zhu H, Wang S, Shan C, et al. Mechanism of protective effect of xuan-bai-cheng-qi decoction on LPS-induced acute lung injury based on an integrated network pharmacology and RNA-sequencing approach. *Respir Res*. 2021;22(1):188. doi:10.1186/s12931-021-01781-1
28. Mao Z, Wang H. Effects of Xuanbai Chengqi decoction on lung compliance for patients with exogenous pulmonary acute respiratory distress syndrome. *Drug Des Devel Ther*. 2016;10:793–798. doi:10.2147/DDDT.S93165
29. Wang Z, Fang K, Wang G, et al. Protective effect of amygdalin on epithelial-mesenchymal transformation in experimental chronic obstructive pulmonary disease mice. *Phytother Res*. 2019;33(3):808–817. doi:10.1002/ptr.6274
30. D'Hulst AI, Vermaelen KY, Brusselle GG, Joos GF, Pauwels RA. Time course of cigarette smoke-induced pulmonary inflammation in mice. *Eur Respir J*. 2005;26(2):204–213. doi:10.1183/09031936.05.00095204
31. Yoshida T, Tuder RM. Pathobiology of cigarette smoke-induced chronic obstructive pulmonary disease. *Physiol Rev*. 2007;87(3):1047–1082. doi:10.1152/physrev.00048.2006
32. Shin NR, Ko JW, Park SH, et al. Protective effect of HwangRyunHaeDok-Tang water extract against chronic obstructive pulmonary disease induced by cigarette smoke and lipopolysaccharide in a mouse model. *J Ethnopharmacol*. 2017;200:60–65. doi:10.1016/j.jep.2017.02.027
33. Cheng Q, Fang L, Feng D, et al. Memantine ameliorates pulmonary inflammation in a mice model of COPD induced by cigarette smoke combined with LPS. *Biomed Pharmacother*. 2019;109:2005–2013. doi:10.1016/j.biopha.2018.11.002
34. Zhu K, Zhou S, Xu A, et al. Microbiota imbalance contributes to COPD deterioration by enhancing IL-17a production via miR-122 and miR-30a. *Mol Ther Nucleic Acids*. 2020;22:520–529. doi:10.1016/j.omtn.2020.09.017
35. Su Y, Han W, Giraldo C, De li Y, Block ER. Effect of cigarette smoke extract on nitric oxide synthase in pulmonary artery endothelial cells. *Am J Respir Cell Mol Biol*. 1998;19(5):819–825. doi:10.1165/ajrcmb.19.5.3091
36. Amano H, Murata K, Matsunaga H, et al. p38 Mitogen-activated protein kinase accelerates emphysema in mouse model of chronic obstructive pulmonary disease. *J Recept Signal Transduct Res*. 2014;34(4):299–306. doi:10.3109/10799893.2014.896380
37. Nair AB, Jacob S. A simple practice guide for dose conversion between animals and human. *J Basic Clin Pharm*. 2016;7(2):27–31. doi:10.4103/0976-0105.177703
38. Huang J, Huang X, Chen Z, Zheng Q, Sun R. Dose conversion among different animals and healthy volunteers in pharmacological study. *Chin J Clin Pharmacol Ther*. 2004;9(9):1069.
39. Zhang W, Li Q, Li D, Li J, Aki D, Liu YC. The E3 ligase VHL controls alveolar macrophage function via metabolic-epigenetic regulation. *J Exp Med*. 2018;215(12):3180–3193. doi:10.1084/jem.20181211
40. Benjamini Y, Hochberg Y. Controlling the false discovery rate: a practical and powerful approach to multiple testing. *J R Stat Soc Series B Stat Methodol*. 1995;57(1):289–300.
41. Knochelmann HM, Dwyer CJ, Bailey SR, et al. When worlds collide: th17 and Treg cells in cancer and autoimmunity. *Cell Mol Immunol*. 2018;15(5):458–469. doi:10.1038/s41423-018-0004-4
42. Luo AN, Leach ST, Barres R, Hesson LB, Grimm MC, Simar D. The microbiota and epigenetic regulation of T helper 17/regulatory T cells: in search of a balanced immune system. *Front Immunol*. 2017;8. doi:10.3389/fimmu.2017.00008
43. Vlahos R, Bozinovski S. Recent advances in pre-clinical mouse models of COPD. *Clin Sci (Lond)*. 2014;126(4):253–265. doi:10.1042/CS20130182
44. Kwan HY, Maddocks M, Nolan CM, et al. The prognostic significance of weight loss in chronic obstructive pulmonary disease-related cachexia: a prospective cohort study. *J Cachexia Sarcopenia Muscle*. 2019;10(6):1330–1338. doi:10.1002/jcsm.12463

45. Dransfield MT, Kunisaki KM, Strand MJ, et al. Acute exacerbations and lung function loss in smokers with and without chronic obstructive pulmonary disease. *Am J Respir Crit Care Med.* 2017;195(3):324–330. doi:10.1164/rccm.201605-1014OC
46. Chu X, Wei M, Yang X, et al. Effects of an anthraquinone derivative from *Rheum officinale* Baill, emodin, on airway responses in a murine model of asthma. *Food Chem Toxicol.* 2012;50(7):2368–2375. doi:10.1016/j.fct.2012.03.076
47. Zhang K, Jiao XF, Li JX, Wang XW. Rhein inhibits lipopolysaccharide-induced intestinal injury during sepsis by blocking the toll-like receptor 4 nuclear factor-kappaB pathway. *Mol Med Rep.* 2015;12(3):4415–4421. doi:10.3892/mmr.2015.3925
48. Lee HS, Jeong GS. Chrysophanol attenuates manifestations of immune bowel diseases by regulation of colorectal cells and T cells activation in vivo. *Molecules.* 2021;26(6):1682. doi:10.3390/molecules26061682
49. Yang HY, Chang HK, Lee JW, et al. Amygdalin suppresses lipopolysaccharide-induced expressions of cyclooxygenase-2 and inducible nitric oxide synthase in mouse BV2 microglial cells. *Neurol Res.* 2007;29(Suppl 1):S59–64. doi:10.1179/016164107X172248
50. Lang GP, Li C, Han YY. Rutin pretreatment promotes microglial M1 to M2 phenotype polarization. *Neural Regen Res.* 2021;16(12):2499–2504. doi:10.4103/1673-5374.313050
51. Ma C, Jiang Y, Zhang X, Chen X, Liu Z, Tian X. Isoquercetin ameliorates myocardial infarction through anti-inflammation and anti-apoptosis factor and regulating TLR4-NF-κB signal pathway. *Mol Med Rep.* 2018;17(5):6675–6680. doi:10.3892/mmr.2018.8709
52. Kim KH, Song -H-H, Ahn K-S, Oh S-R, Sadikot RT, Joo M. Ethanol extract of the tuber of *Alisma orientale* reduces the pathologic features in a chronic obstructive pulmonary disease mouse model. *J Ethnopharmacol.* 2016;188:21–30. doi:10.1016/j.jep.2016.05.004
53. Ghebre MA, Pang PH, Diver S, et al. Biological exacerbation clusters demonstrate asthma and chronic obstructive pulmonary disease overlap with distinct mediator and microbiome profiles. *J Allergy Clin Immunol.* 2018;141(6):2027–2036.e2012. doi:10.1016/j.jaci.2018.04.013
54. Chakrabarti S, Patel KD. Matrix metalloproteinase-2 (MMP-2) and MMP-9 in pulmonary pathology. *Exp Lung Res.* 2005;31(6):599–621. doi:10.1080/019021490944232
55. Greenlee KJ, Werb Z, Kheradmand F. Matrix metalloproteinases in lung: multiple, multifarious, and multifaceted. *Physiol Rev.* 2007;87(1):69–98. doi:10.1152/physrev.00022.2006
56. Kumar M, Bhadoria DP, Dutta K, et al. Combinatorial effect of TIMP-1 and alpha1AT gene polymorphisms on development of chronic obstructive pulmonary disease. *Clin Biochem.* 2011;44(13):1067–1073. doi:10.1016/j.clinbiochem.2011.06.986
57. Abd E-FM-F, Ghazy MA, Mostafa MS, El-Attar MM, Osman A. Identification of MMP-9 as a biomarker for detecting progression of chronic obstructive pulmonary disease. *Biochem Cell Biol.* 2015;93(6):541–547. doi:10.1139/bcb-2015-0073
58. Budden KF, Gellatly SL, Wood DLA, et al. Emerging pathogenic links between microbiota and the gut-lung axis. *Nat Rev Microbiol.* 2017;15(1):55–63. doi:10.1038/nrmicro.2016.142
59. Man WH, de Steenhuijsen Piters WA, Bogaert D. The microbiota of the respiratory tract: gatekeeper to respiratory health. *Nat Rev Microbiol.* 2017;15(5):259–270. doi:10.1038/nrmicro.2017.14
60. Le Bourvellec C, Boas PBV, Lepercq P, et al. Procyanidin-cell wall interactions within apple matrices decrease the metabolism of procyanidins by the human gut microbiota and the anti-inflammatory effect of the resulting microbial metabolome in vitro. *Nutrients.* 2019;11(3):664. doi:10.3390/nu11030664
61. Hu L, Jin L, Xia D, et al. Nitrate ameliorates dextran sodium sulfate-induced colitis by regulating the homeostasis of the intestinal microbiota. *Free Radic Biol Med.* 2020;152:609–621. doi:10.1016/j.freeradbiomed.2019.12.002
62. Opstelten JL, Plassais J, van Mil SWC, et al. Gut microbial diversity is reduced in smokers with Crohn's disease. *Inflamm Bowel Dis.* 2016;22(9):2070–2077. doi:10.1097/MIB.0000000000000875
63. Pujo J, Petitfils C, Le Faouder P, et al. Bacteria-derived long chain fatty acid exhibits anti-inflammatory properties in colitis. *Gut.* 2021;70(6):1088–1097. doi:10.1136/gutjnl-2020-321173
64. Ruocco C, Ragni M, Rossi F, et al. Manipulation of dietary amino acids prevents and reverses obesity in mice through multiple mechanisms that modulate energy homeostasis. *Diabetes.* 2020;69(11):2324–2339. doi:10.2337/db20-0489
65. Zhao JB, Liu P, Wu Y, et al. Dietary fiber increases butyrate-producing bacteria and improves the growth performance of weaned piglets. *J Agr Food Chem.* 2018;66(30):7995–8004. doi:10.1021/acs.jafc.8b02545
66. Zheng DP, Liwinski T, Elinav E. Interaction between microbiota and immunity in health and disease. *Cell Res.* 2020;30(6):492–506. doi:10.1038/s41422-020-0332-7
67. Ansaldo E, Farley TK, Belkaid Y. Control of immunity by the microbiota. *Annu Rev Immunol.* 2021;39:449–479. doi:10.1146/annurev-immunol-093019-112348
68. Michalovich D, Rodriguez-Perez N, Smolinska S, et al. Obesity and disease severity magnify disturbed microbiome-immune interactions in asthma patients. *Nat Commun.* 2019;10(1):5711. doi:10.1038/s41467-019-13751-9
69. Wang Z, Maschera B, Lea S, et al. Airway host-microbiome interactions in chronic obstructive pulmonary disease. *Respir Res.* 2019;20(1):113. doi:10.1186/s12931-019-1085-z
70. Wright JL, Churg A. Animal models of cigarette smoke-induced COPD. *Chest.* 2002;122(6 Suppl):301S–306S. doi:10.1378/chest.122.6\_suppl.301S
71. Limjunyawong N, Craig JM, Lagasse HAD, Scott AL, Mitzner W. Experimental progressive emphysema in BALB/cJ mice as a model for chronic alveolar destruction in humans. *Am J Physiol-Lung C.* 2015;309(7):L662–L676. doi:10.1152/ajplung.00214.2015

### Publish your work in this journal

The International Journal of COPD is an international, peer-reviewed journal of therapeutics and pharmacology focusing on concise rapid reporting of clinical studies and reviews in COPD. Special focus is given to the pathophysiological processes underlying the disease, intervention programs, patient focused education, and self management

protocols. This journal is indexed on PubMed Central, MedLine and CAS. The manuscript management system is completely online and includes a very quick and fair peer-review system, which is all easy to use. Visit <http://www.dovepress.com/testimonials.php> to read real quotes from published authors.